Applied Mathematics & Information Sciences
An International Journal

http://dx.doi.org/10.12785/amis/090314

The Magnetic Field of Electrical Conducting Sheets with Two Non-Overlapping Insertions

D. M. El-Sakout, A. F. Ghaleb[*]*, M. S. Abou-Dina and A. A. Ashour*

Department of Mathematics, Faculty of Science, Cairo University, Giza 12613, Egypt

Received: 15 Jul. 2014, Revised: 16 Oct. 2014, Accepted: 17 Oct. 2014
Published online: 1 May 2015

Abstract: Generalizing a previous result by two of the authors (MSA and AAA) for an infinite sheet with one insertion, we derive two coupled linear Fredholm integral equations of the second kind on two coplanar contours for the determination of the magnetic field due to an infinite plane electrical conducting sheet with two non-overlapping insertions, permeated by a uniform, parallel electric field. These equations are solved numerically to provide solutions for new problems involving two elliptic insertions. The level lines for the current function in the sheet are plotted and the results are discussed to assess the efficiency of the numerical method. The conclusions are relevant to non-destructive testing of electrical conducting sheets and to the evaluation of magnetic fields on the earth's surface around islands. Generalization to any finite number of insertions is straightforward.

Keywords: Electrical conducting sheet, insertion, inhomogeneous electrical conductivity, current function, boundary integral method, non-destructive testing

1 Introduction

The problem of excitation of electric currents and magnetic fields in non-uniform electrical conducting sheets by electric fields has many applications. In Technology, the holes, the islands and the adhesives in metallic chips used in industry may considerably affect the performance of these chips, and the correct determination of the magnetic field variations due to such insertions is of primordial interest in non-destructive testing. In Geophysics, the solar eclipses and meteors may affect the electrical conductivity in large areas of the Earth's surface and thus create unwanted magnetic disturbances. Also, the islands in the vast ocean may be modeled as inclusions of different electrical conductivity in an infinite water current sheet. Due to its importance, this topic was investigated since many decades. Ashour and Chapman [1] found the components of the magnetic field due to an infinite plane current sheet of uniform conductivity, except for a circular disc of different uniform conductivity, placed in an initially uniform, parallel electric field. The elliptic insertion was also considered, but the components of the additional magnetic field could not be obtained due to the complexity of the formulae. The same authors [2] investigated the sudden creation of conductivity in connection with what is known as the meteor geomagnetic effects. Ashour [3] investigated induction in finite thin sheets. Later on, Ashour [4] generalized previous work to cover any number of insertions with arbitrary boundaries, and obtained the additional magnetic field as a summation of linear integrals along these boundaries. The integrand in each integral involves only a certain combination of the limiting values of the electric potential at both sides of the corresponding boundary. The author applied this idea to solve the case of an elliptic insertion, but the problem remained partially unsolved. In [5] Ashour solved the problem of two non-overlapping circular insertions and presented numerical results when the insertions have zero electrical conductivity. According to this formulation, if a certain combination of the boundary values of the additional electric potential is known, then one may find the components of the additional magnetic field everywhere in space without recurring to the solution of Laplace's equation. Abou-Dina and Ashour [6] took an important step towards the complete resolution of the problem for one insertion of arbitrary shape by deriving a linear Fredholm integral equation of the second kind on a plane contour which divides the infinite plane conducting sheet

[*] Corresponding author e-mail: afghaleb@sci.cu.edu.eg

into two regions of different uniform conductivities. This integral equation admits exact solutions in closed form for the cases of circular or elliptic insertions, and its numerical solution for arbitrarily shaped boundaries allows to resolve the problem completely within boundary techniques. The authors applied the method to a square insertion of zero electrical conductivity. Exact solutions for other two-dimensional problems of induction in thin non-uniform sheets were considered in [7]. The numerous advantages of the boundary integral techniques were recognized long ago. In the past few decades, these methods acquired even more interest as they could be easily implemented for rather arbitrary shapes of the domain of solution. In the numerical solution of boundary-value problems by integral equation methods, the main sources of error reside in the approximation of the contour by a broken line, and in the application of the resulting discretized integral equation at only a finite number of points. In spite of this, the obtained numerical results are generally accurate enough. Like in many other branches such as the Theory of Elasticity or Hydrodynamics, the use of boundary integral techniques found wide application in solving linear and nonlinear electrostatic problems. Cade [8] studies a general two-dimensional electrostatic system consisting of any finite number of conducting and dielectric bodies whose surfaces are circular cylinders each outside of the others, influenced by an arbitrary given field. The system is described by a set of simultaneous integral equations, in which the unknown functions are the densities of the induced electric charges on the surfaces of the conductors. This work generalizes previous investigations by Durand. Sellier [9] uses boundary integrals to solve the problem of a slender dielectric body embedded in an arbitrary external potential. Shail [10] and Cade ([8], [11]) investigate the problem of a slender torus. The discontinuous solutions of the integral equations of electrostatics are discussed by Cade [12]. The use of integral equations in three-dimensional modeling of electromagnetism is investigated in [13]. There is abundant literature about non-uniform electrical conducting sheets and the mathematical methods used in resolving such problems, especially when the external field is time dependent. We briefly quote here some of these references for geophysical applications and in Technology, mainly in the field of non-destructive testing of metal sheets: [3], [14], [15], [7], [16], [17], [18], [19], [20], [21]. The present paper is devoted to the study of infinite electrical conducting plane sheets with non-homogeneous electrical conductivity, permeated by a uniform, parallel electric field. More precisely, the sheet is assumed to have homogeneous conductivity everywhere, except for two ”islands” of different uniform conductivities and arbitrary shapes. The problem is resolved for the current function and the additional magnetic field components within a boundary integral formulation developed earlier for one inclusion, thus avoiding the solution of Laplace’s equation in space. The results may be easily generalized to any finite number of insertions. The paper is organized into five sections and an appendix: Section 1 is an introduction about the history of the problem and the organization of the paper; Section 2 is devoted to the description of the mathematical model; in Section 3 we present the main integral formulae for the calculation of the current function in the sheet and the magnetic field components in space, in terms of two unknown functions defined on the boundaries of the inclusions; in Section 4 we derive the basic coupled integral equations satisfied by the two unknown boundary functions; Section 5 concerns the applications, with numerical results and discussion. In the appendix we have shown the details of the derivation of the basic coupled integral equations.

2 Mathematical problem

We consider an infinite plane current sheet given by $z = 0$ in the system of Cartesian coordinates $O(x,y,z)$. Closed contours C_1 and C_2 with parametric equations $x = x(s)$, $y = y(s)$ and $x = x(\tau)$, $y = y(\tau)$ respectively where s and τ denotes the arc lengths on C_1 and C_2 respectively, divide the plane into three regions: The interiors D_1 , D_2 and the exterior D_0. The conductivities in the three regions are uniform and equal to σ_1, σ_2 and σ_0 respectively.
A uniform electric field **E** parallel to the plane of the sheet excites electric currents in the sheet. Let this electric field be inclined at an angle α to the x-axis. Then

$$\mathbf{E} = E(\cos\alpha\mathbf{i} + \sin\alpha\mathbf{j})$$

where **i**, **j**, **k** denote the unit vectors in the directions of increasing of x, y, z respectively.

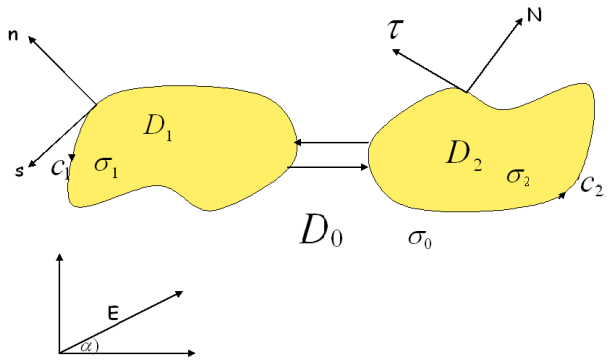

Fig. 1: Geometry of the problem.

It is required to evaluate the components of the resulting magnetic field. We shall denote by $\psi^0(x,y)$ the current function of the undisturbed current flow if the whole sheet were of integrated conductivity σ_0 and by

$V_m^0(x,y)$ the electric potential that would be required to maintain this undisturbed current flow in the non-uniform sheet. Hence

$$\begin{aligned} \psi^0(x,y) &= I[x\sin\alpha - y\cos\alpha] \\ V_m^0(x,y) &= -I\sigma_m^{-1}[x\cos\alpha + y\sin\alpha] \end{aligned} \tag{1}$$

corresponding to the area D_m, $m = 0,1,2$ and $I = \sigma_0 E$. The additional current function and additional electric potential are denoted respectively ψ_m, V_m in D_m. The total current function and electric potential are $\psi_m^{'}$, $V_m^{'}$ respectively. In D_m

$$\begin{aligned} \psi_m^{'}(x,y) &= \psi^0(x,y) + \psi_m(x,y) \\ V_m^{'} &= V_m^0(x,y) + V_m(x,y). \end{aligned} \tag{2}$$

From the theory of uniform current sheets it is known that $V_m^{'}(x,y)$, $\psi_m^{'}(x,y)$, $\psi_m(x,y)$ and $V_m(x,y)$ satisfy the two-dimensional Laplace's equation in the area D_m.

For a general point in D_m

$$\mathbf{k} \times grad\, \psi_m^{'} = -\sigma_m grad\, V_m^{'}$$

$$\mathbf{k} \times grad\, \psi_m = -\sigma_m grad\, V_m.$$

The boundary conditions for $\psi_m^{'}(x,y)$ express the continuity of $\psi_m^{'}(x,y)$ and $\sigma_m^{-1}\frac{\partial}{\partial n}\psi_m^{'}(x,y)$ (the tangential components of the electric field) at the boundary C_1, $m = 0,1$, the continuity of $\psi_m^{'}(x,y)$ and $\sigma_m^{-1}\frac{\partial}{\partial N}\psi_m^{'}(x,y)$ (the tangential components of the electric field) at the boundary C_2, $m = 0,2$ and the vanishing of $\psi^0(x,y)$ at infinite distance from this boundary.

The boundary conditions for $V_m^{'}(x,y)$ express the continuity of $V_m^{'}(x,y)$ and of $\sigma_m\frac{\partial}{\partial n}V_m^{'}(x,y)$ (the normal components of the current density)at the boundary of C_1, $m = 0,1$, the continuity of $V_m^{'}(x,y)$ and of $\sigma_m\frac{\partial}{\partial N}V_m^{'}(x,y)$ (the normal components of the current density) at the boundary of C_2, $m = 0,2$ and the vanishing of $V_0(x,y)$ at infinite distances from the boundary. The directional derivatives in the plane of the sheet along the normal and tangent directions are $\frac{\partial}{\partial n}$ and $\frac{\partial}{\partial s}$ respectively on the boundary C_1, the corresponding quantities on the boundary C_2 are $\frac{\partial}{\partial N}$ and $\frac{\partial}{\partial \tau}$ respectively.

3 Current function and additional magnetic field

Extending Ashour's result [5] in an obvious way, one may write down the following expression for the magnetic scalar potential $\Omega(x,y,z)$ of the additional system of currents due to the above insertions, calculated at a field point $P(x,y,z)$ in the half-space $z \geq 0$:

$$\begin{aligned} \Omega(x,y,z) = -[&\oint_{C_1} log(R_1+z)\frac{d}{ds}G_1(s)ds \\ &+ \oint_{C_2} log(R_2+z)\frac{d}{d\tau}G_2(\tau)d\tau], \end{aligned} \tag{3}$$

where R_1, R_2 are the distances between the field point P and the boundary points $q_1 = (x(s),y(s),0)$, $q_2 = (x(\tau),y(\tau),0)$:

$$R_1 = \sqrt{(x-x(s))^2 + (y-y(s))^2 + z^2}$$

$$R_2 = \sqrt{(x-x(\tau))^2 + (y-y(\tau))^2 + z^2}$$

The following notations were introduced for convenience:

$$F_1(s) = \frac{dG_1(s)}{ds}, \qquad F_2(\tau) = \frac{dG_2(\tau)}{d\tau}, \tag{4}$$

$$\begin{aligned} G_1(s) &= \sigma_1 V_1^{C_1}(s) - \sigma_0 V_0^{C_1}(s) \\ G_2(\tau) &= \sigma_2 V_2^{C_2}(\tau) - \sigma_0 V_0^{C_2}(\tau), \end{aligned} \tag{5}$$

$V_1^{C_1}(s)$, $V_2^{C_2}(\tau)$, $V_0^{C_1}(s)$ and $V_0^{C_2}(\tau)$ are the limiting values of the electric potential at the boundaries C_1 and C_2. According to our definition, the current function $\psi(x,y)$ in the sheet may be calculated from the theory of thin current sheets [1] as the negative double of the jump of the magnetic potential across the sheet when moving along the positive sense of the z-axis. Because of obvious symmetry, this may be written as:

$$\psi(x,y) = -2\Omega(x,y,0+). \tag{6}$$

The expressions for the magnetic field components are:

$$\begin{aligned} H_x(x,y,z) = -\frac{\partial\Omega}{\partial x} = &\oint_{C_1} \frac{x-x(s)}{R_1(R_1+z)}F_1(s)ds \\ &+ \oint_{C_2} \frac{x-x(\tau)}{R_2(R_2+z)}F_2(\tau)d\tau, \end{aligned} \tag{7}$$

$$\begin{aligned} H_y(x,y,z) = -\frac{\partial\Omega}{\partial y} = &\oint_{C_1} \frac{y-y(s)}{R_1(R_1+z)}F_1(s)ds \\ &+ \oint_{C_2} \frac{y-y(\tau)}{R_2(R_2+z)}F_2(\tau)d\tau, \end{aligned} \tag{8}$$

$$H_z(x,y,z) = -\frac{\partial\Omega}{\partial z} = \oint_{C_1} \frac{F_1(s)}{R_1}ds + \oint_{C_2} \frac{F_2(\tau)}{R_2}d\tau. \tag{9}$$

These last four relations allow to evaluate the current function in the sheet and the magnetic field components everywhere in space, once the functions $F_1(s)$ and $F_2(\tau)$ have been determined. The next section is devoted to the derivation of the coupled boundary integral equations satisfied by these two functions.

4 The basic coupled integral equations

The two functions $V_m(x,y)$ and $\sigma_m^{-1}\psi_m(x,y)$ are harmonic and satisfy the Cauchy-Riemann relations in the simply connected domain D_m, $m = 1,2$. This implies that

$V_m(x,y)+i\sigma_m^{-1}\psi_m(x,y)$ is an analytical function of the complex variable. From the Cauchy integral theorem:

$$V_1(x,y)+i\sigma_1^{-1}\psi_1(x,y) = \frac{1}{2\pi i}\oint_{C_1}\frac{V_1^{C_1}(s')+i\sigma_1^{-1}\psi_1^{C_1}(s')}{q_1-p}dq_1,$$

where

$$q_1 = x(s')+iy(s') \qquad p = x(s)+iy(s)$$

p is a field point inside the insertion and

$$q_1-p = r_{11}e^{i\theta_{11}}.$$

Therefore,

$$\frac{dq_1}{q_1-p} = d(\log(q_1-p)) = \frac{\partial}{\partial s'}(\log r_{11}+i\theta_{11})ds',$$

where ds' denotes the differential length along the contour C_1 at the boundary point $(x(s'),y(s'))$. Hence

$$V_1(x,y) = \frac{1}{2\pi}\oint_{C_1}[V_1^{C_1}(s')\frac{\partial \log r_{11}}{\partial n'}+\frac{1}{\sigma_1}\psi_1^{C_1}(s')\frac{\partial \log r_{11}}{\partial s'}]ds'.$$

when p lies on the contour C_1,

$$V_1^{C_1}(s) = \frac{1}{\pi}\oint_{C_1}[V_1^{C_1}(s')\frac{\partial \log r_{11}}{\partial n'} +\frac{1}{\sigma_1}\psi_1^{C_1}(s')\frac{\partial \log r_{11}}{\partial s'}]ds', \quad (10)$$

with

$$r_{11} = \sqrt{(x(s)-x(s'))^2+(y(s)-y(s'))^2}.$$

Similarly, one derives the expression

$$V_2^{C_2}(\tau) = \frac{1}{\pi}\oint_{C_2}[V_2^{C_2}(\tau')\frac{\partial}{\partial N'}\log r_{22} +\frac{1}{\sigma_2}\psi_2^{C_2}(\tau')\frac{\partial}{\partial \tau'}\log r_{22}]d\tau', \quad (11)$$

with

$$r_{22} = \sqrt{(x(\tau)-x(\tau'))^2+(y(\tau)-y(\tau'))^2}.$$

It will be shown in Appendix that the basic coupled integral equations for the functions F_1 and F_2 assume the form:

$$F_1(s)-\frac{\sigma_0-\sigma_1}{\pi(\sigma_0+\sigma_1)}[\oint_{C_1}F_1(s')\frac{\partial \log r_{11}}{\partial n}ds' +\oint_{C_2}F_2(\tau')\frac{\partial \log r_{12}}{\partial n}d\tau'] = \frac{2(\sigma_0-\sigma_1)}{\sigma_0+\sigma_1}I[\dot{x}(s)\cos\alpha+\dot{y}(s)\sin\alpha], \quad (12)$$

$$F_2(\tau)-\frac{\sigma_0-\sigma_2}{\pi(\sigma_0+\sigma_2)}[\oint_{C_1}F_1(s')\frac{\partial \log r_{21}}{\partial N}ds' +\oint_{C_2}F_2(\tau')\frac{\partial \log r_{22}}{\partial N}d\tau'] = \frac{2(\sigma_0-\sigma_2)}{\sigma_0+\sigma_2}I[\dot{x}(\tau)\cos\alpha+\dot{y}(\tau)\sin\alpha], \quad (13)$$

where

$$r_{11} = \sqrt{(x(s)-x(s'))^2+(y(s)-y(s'))^2},$$

$$r_{12} = \sqrt{(x(s)-x(\tau'))^2+(y(s)-y(\tau'))^2},$$

$$r_{21} = \sqrt{(x(\tau)-x(s'))^2+(y(\tau)-y(s'))^2},$$

$$r_{22} = \sqrt{(x(\tau)-x(\tau'))^2+(y(\tau)-y(\tau'))^2}.$$

The obtained formulae were tested in different ways: First, we have set $\sigma_0=\sigma_2$. It follows that $F_2(\tau)=0$ as may be directly verified, and the one-insertion case treated in [6] is recovered. Numerical tests were carried out for this case and the previous known results for one circular, elliptic or square insertion were all recovered with high precision. Second, we have exactly recovered the numerical results for two circular insertions treated in [5]. Also, although the basic equations and the proofs presented above do not allow the vanishing of the electrical conductivity of an island, one easily verifies that the obtained pair of coupled integral equations remains valid in the limit when σ_1 and/or σ_2 tend to zero, which means that our final results can be used to treat the cases of practical importance when the insertions are poor conductors, or even holes.

5 Numerical results and discussion

For conciseness, we consider in what follows only one geometry, involving two elliptic insertions with parallel or perpendicular major axes. The case of two slots is also investigated as a special case of the ellipse, as the eccentricity is close to unity. To the best of our knowledge, the obtained results are new and clearly indicate that the proposed formulation may be effectively used to solve difficult boundary-value problems in this area of research. In each case, the two boundaries have been discretized in the usual way by defining point partitions on them. The coupled integral equations were thus reduced to a system of linear algebraic equations and the functions $F(s),F(\tau)$ were evaluated numerically at the chosen set of boundary points. The obtained values were then used in conjunction with Fourier expansion to obtain analytic expressions for the two functions. These are subsequently fed into the integrals for the total current function and for the components of the magnetic field to produce numerical results and plots. As the used Fourier expansions were taken in complex form, the number of

points on each boundary was chosen odd. Only two settings have been used for definiteness, for which the axes are such that the applied electric field is directed either along the x-axis $(\alpha = 0)$ or along the y-axis $(\alpha = \pi/2)$. The magnetic field components are related to the characteristic magnetic field H_0 of the undisturbed current flow in the non-homogeneous sheet, defined by:

$$H_0 = \frac{I}{2}.$$

These components have been plotted for three values of the z-coordinate:

$$z = 0; 0.5; 1.$$

The corresponding curves are labeled 1; 2; 3 respectively. In the presented figures for the level lines of the total current function, it is noticed that the current lines are denser in the insertion with electrical conductivity larger than that of the host matrix and the current lines are attracted towards the insertion, the converse being true for the insertion with lower electrical conductivity. Also, the additional magnetic field tends to zero as one gets further away from the insertions. Inside the insertions, when the level curves for the total current function are close to being equally distanced straight lines, the component of the magnetic field in the direction perpendicular to these lines will be almost constant, as appears from the figures. All these results are expected on a physical basis, and provide an indication to the correctness of the calculations.

It is important to notice the existence of singular behavior of solutions for the magnetic field components at boundaries of discontinuity of the function of electrical conductivity, even within the used linearized theory of Electromagnetism. These may be weak singularities, jumps or infinite discontinuities of logarithmic nature as appears on the different plots. The logarithmic singularity may be put in evidence by considering the boundary integral expression (9) for the magnetic field component perpendicular to the sheet. After substituting into it the Fourier expansion for F_i, this expression is seen to involve an elliptic integral of the third kind, which is known to have a logarithmic singularity (cf. [22], p.303). Such a singularity is clearly unrealistic, it is only a result of the inadequacy of the used model in regions of the sheet contiguous to the boundaries.

The calculations were successfully performed on a multitude of geometries, smooth boundaries or boundaries with corner points, and for a number of settings of the applied electric field. Only the following three cases are presented:

A. **Two elliptic insertions with parallel major axes.** The ellipses have same dimensions, major axis half-length equal to unity, eccentricity $e \simeq 0.94$. The centers of the ellipses lie on the y-axis, with major axes aligned perpendicular to the direction of the initial electric field $(\alpha = \frac{\pi}{2})$ and are a distance apart equal to double the length of the major axis. The electrical conductivities take the values such that:

$$\frac{\sigma_1}{\sigma_0} = 1.5, \qquad \frac{\sigma_2}{\sigma_0} = 0.75.$$

Figure 2 shows the corresponding level curves for the total current function. Figure 3 displays the magnetic

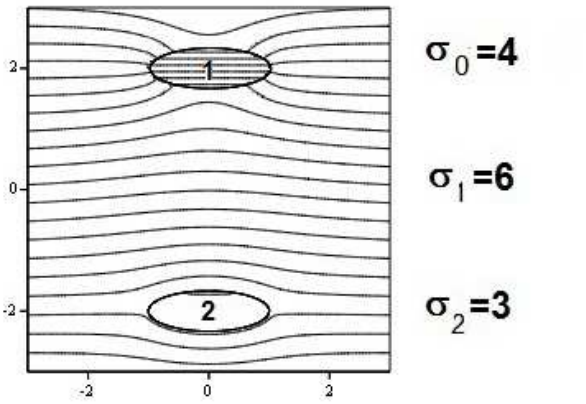

Fig. 2: Level lines for the total current function for two elliptic insertions: Symmetric setting with major axes parallel to the direction of the applied electric field and line of centers perpendicular to this direction.

field components H_x, H_y and H_z as functions of x for $y = 0$, i.e. when the observer moves along a path parallel to the major axes in the direction of the applied electric field and symmetrically positioned with respect to the two insertions. The symmetry properties in these figures are obvious and may be used experimentally to determine the side in which the insertion of high (low) electrical conductivity lies. Comparison between the components shows that the maximum absolute value of the component H_y is much smaller than that of the other two components. Thus the components H_y and H_y may be more appropriate for measurements. Figure 4 shows the magnetic field components H_y and and H_z as functions of y for $x = 0$, i.e. when the observer moves along a direction parallel to the line of centers, perpendicular to the direction of the applied field. The crossing of the two boundaries takes place when $z = 0$ and is accompanied by a weak discontinuity in H_y and an infinite discontinuity in H_z. The field inside the insertions is linear, nearly constant. The locations of the discontinuities may be used for the determination

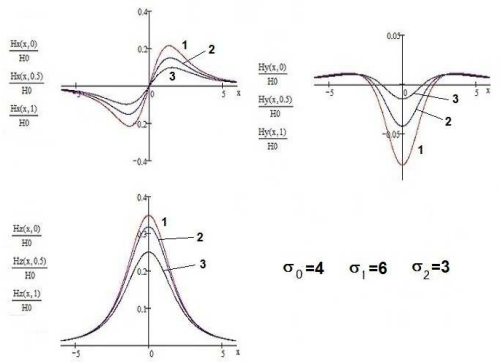

Fig. 3: Magnetic field components H_x, H_y and H_z as functions of x, for $y = 0$ for two elliptic insertions: Symmetric setting with major axes parallel to the direction of the applied electric field and line of centers perpendicular to this direction.

of the locations of the insertions from measurements of these magnetic field components.

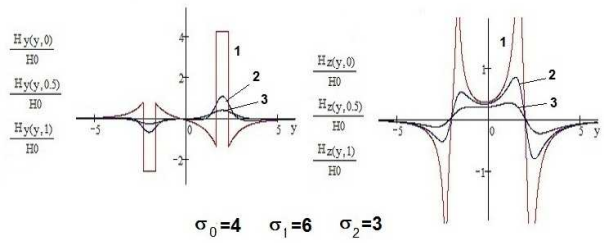

Fig. 4: Magnetic field components H_y and H_z as functions of y, for $x = 0$ for two elliptic insertions: Symmetric setting with major axes parallel to the direction of the applied electric field and line of centers perpendicular to this direction.

B.**Two parallel elliptic slots.** The ellipses have same dimensions, major axis half-length equal to unity, eccentricity $e \simeq 0.99$, rendering the ellipses very thin. The centers of the ellipses lie on the y-axis, with major axes aligned perpendicular to the direction of the initial electric field $(\alpha = \frac{\pi}{2})$ and are a distance apart equal to double the length of the major axis. The electrical conductivities take the values such that:

$$\frac{\sigma_1}{\sigma_0} = 1.25, \qquad \frac{\sigma_2}{\sigma_0} = 0.50.$$

The level curves for the total current function in this case are represented on Figure 5.
The curves for the magnetic field components as functions of x for $y = 0$ are shown on Figure 6.

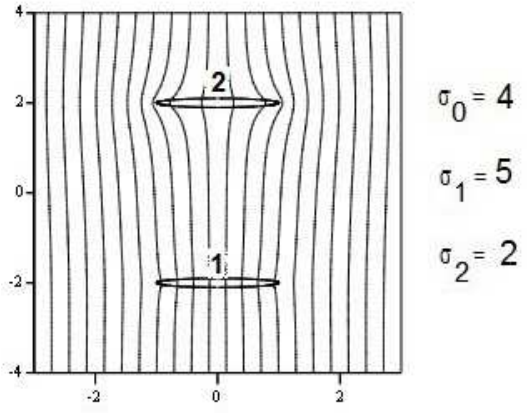

Fig. 5: Level lines for the total current function for two slots: Symmetric setting with major axes perpendicular to the direction of the applied electric field and line of centers parallel to this direction.

Figure 7 displays the magnetic field component H_x as function of y for $x = 0$. The weak discontinuities are evident as the boundaries are crossed.

C.**Two elliptic insertions with perpendicular major axes.** The geometrical parameters of the ellipses are as in case A. The centers lie on the y-axis, the major axis of insertion (2) is parallel to the applied electric field $(\alpha = 0)$, the major axis of insertion (1) is perpendicular to this direction. The electrical conductivities satisfy

$$\frac{\sigma_1}{\sigma_0} = 1.2, \qquad \frac{\sigma_2}{\sigma_0} = 0.80.$$

The level curves for the total current function are shown on Figure 9. We have represented on Figure 10 the magnetic field component H_y, and on Figure 11 the field component H_z, both as functions of y for $x = 0$. The singular behavior of these two components is clear at those points where the y-axis intersects the boundaries of the ellipses.

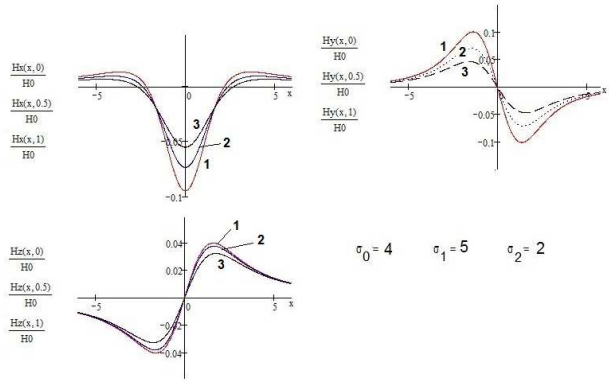

Fig. 6: Magnetic field components H_x, H_y and H_z as functions of x, for $y = 0$ for two slots: Symmetric setting with major axes perpendicular to the direction of the applied electric field and line of centers parallel to this direction.

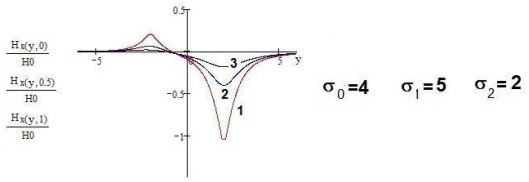

Fig. 7: Magnetic field components H_x as function of y, for $x = 0$ for two slots: Symmetric setting with major axes perpendicular to the direction of the applied electric field and line of centers parallel to this direction.

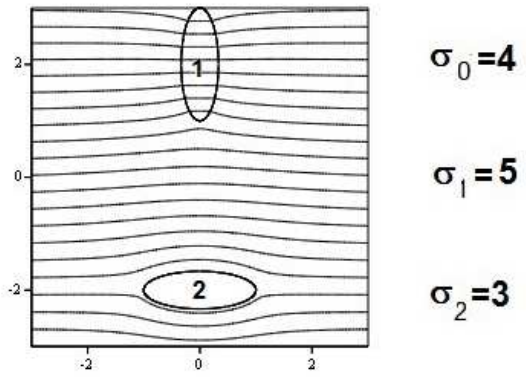

Fig. 8: Level lines for the total current function for two elliptic insertions: One major axis perpendicular to the direction of the applied electric field, the other major axis perpendicular to this direction.

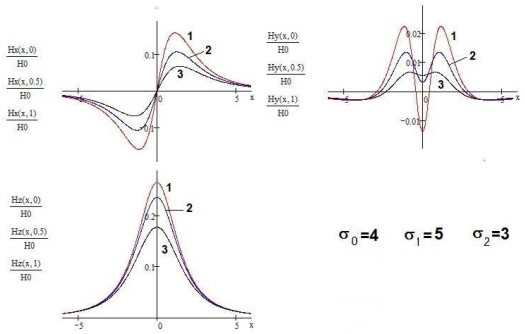

Fig. 9: Magnetic field components H_x, H_y and H_z as functions of x, for $y = 0$, for two elliptic insertions: One major axis perpendicular to the direction of the applied electric field, the other major axis perpendicular to this direction.

The following general remarks are due:

1. All the results are in accordance with the Theory of Electromagnetism in quasi-static formulation.
2. The different components of the electromagnetic field show singular behavior on the sheet, at the boundary points. The singularities may be of weak type, finite jumps or else logarithmic singularities.
3. The presence of logarithmic singularity for the magnetic field component normal to the sheet at the boundary points clearly indicate the inadequacy of the linear model in the regions of the sheet close to the boundaries of the insertions.
4. Although the deduction of the integral equations for the functions F_i requires the electrical conductivities of the insertions to be non zero, the final form of these equations is not subject to such a restriction.
5. The used numerical scheme performed well in almost all cases, whether the insertion is electrical conductor, isolator or even hole. The previous known results were all recovered as special cases. The obtained results provide effective solutions to diffcult, three-dimensional boundary-value problems for Laplace's equation, otherwise impossible to solve analytically.
6. During the calculations, the partitions of the boundaries were gradually refined, till the numerical figures stabilized within the required accuracy. The presented results were obtained with uniform partitions consisting of 101 points. The relative errors were within the limits of 1%.

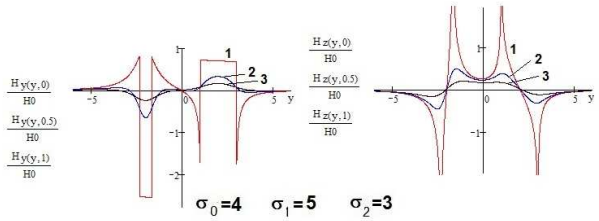

Fig. 10: Magnetic field components H_y and H_z as functions of y, for $x = 0$, for two elliptic insertions: One major axis perpendicular to the direction of the applied electric field, the other major axis perpendicular to this direction.

7. In case of boundary corner points, the corresponding function F_i may have jumps. This will cause Gibb's phenomenon to take place when this function is expanded in a Fourier series. To avoid the resulting errors, the corner should be rounded. This can be achieved either by replacing portions of the boundary by properly chosen curves, or by replacing the whole boundary by another smooth one, or else by just avoiding to include the corner points in the partition.
8. It was noticed that the level curves for the total current function could not be drawn correctly in some cases. Closed contours would appear threading the boundaries, a fact that is not likely to happen in practice. This phenomenon was observed to gradually disappear as the value of the electrical conductivity of the host matrix was increased relative those of the insertions.
9. The results may be directly generalized to the infinite electrical conducting sheet with any finite number of insertions.

Acknowledgement

Thanks are due to the anonymous referees for their careful checking of the work.

Appendix A

The expressions (10) and (11) for $V_1^{C_1}(s)$ and $V_2^{C_2}(\tau)$ may be written as follows:

$$V_1^{C_1}(s) = \frac{1}{\pi}\oint_{C_1}[V_1^{C_1}(s')\frac{\partial \log r_{11}}{\partial n'} + \frac{1}{\sigma_1}\psi_1^{C_1}(s')\frac{\partial \log r_{11}}{\partial s'}]ds' + \frac{1}{\pi}\oint_{C_2}[V_2^{C_2}(\tau')\frac{\partial \log r_{12}}{\partial N'} + \frac{1}{\sigma_2}\psi_2^{C_2}(\tau')\frac{\partial \log r_{12}}{\partial \tau'}]d\tau',$$

$$V_2^{C_2}(\tau) = \frac{1}{\pi}\oint_{C_1}[V_1^{C_1}(s')\frac{\partial \log r_{21}}{\partial n'} + \frac{1}{\sigma_1}\psi_1^{C_1}(s')\frac{\partial \log r_{21}}{\partial s'}]ds' + \frac{1}{\pi}\oint_{C_2}[V_2^{C_2}(\tau')\frac{\partial \log r_{22}}{\partial N'} + \frac{1}{\sigma_2}\psi_2^{C_2}(\tau')\frac{\partial \log r_{22}}{\partial \tau'}]d\tau',$$

because in the first equation the second integral vanishes and in the second equation the first integral vanishes. Also,

$$V_0^{C_1}(s) = -\frac{1}{\pi}\oint_{C_1}[V_0^{C_1}(s')\frac{\partial \log r_{11}}{\partial n'} + \frac{1}{\sigma_0}\psi_0^{C_1}(s')\frac{\partial \log r_{11}}{\partial s'}]ds' - \frac{1}{\pi}\oint_{C_2}[V_0^{C_2}(\tau')\frac{\partial}{\partial N'}\log r_{12} + \frac{1}{\sigma_0}\psi_0^{C_2}(\tau')\frac{\partial}{\partial \tau'}\log r_{12}]d\tau', \quad (14)$$

$$V_0^{C_2}(\tau) = -\frac{1}{\pi}\oint_{C_1}[V_0^{C_1}(s')\frac{\partial \log r_{21}}{\partial n'} + \frac{1}{\sigma_0}\psi_0^{C_1}(s')\frac{\partial \log r_{21}}{\partial s'}])ds' - \frac{1}{\pi}\oint_{C_2}[V_0^{C_2}(\tau')\frac{\partial \log r_{22}}{\partial N'} + \frac{1}{\sigma_0}\psi_0^{C_2}(\tau')\frac{\partial \log r_{22}}{\partial \tau'}]d\tau', \quad (15)$$

with

$$r_{12} = \sqrt{(x(s)-x(\tau'))^2 + (y(s)-y(\tau'))^2},$$

$$r_{21} = \sqrt{(x(\tau)-x(s'))^2 + (y(\tau)-y(s'))^2}.$$

From the continuity of the current function and the electric potential:

$$\psi_0^{C_1}(s) = \psi_1^{C_1}(s),$$

$$\psi_0^{C_2}(\tau) = \psi_2^{C_2}(\tau),$$

$$V_0' = V_1' \quad \text{on} \quad C_1, \qquad V_0' = V_2' \quad \text{on} \quad C_2.$$

From the second of equations (2) applied on C_1

$$V_0^0 + V_0 = V_1^0 + V_1.$$

and from (1) after some manipulations

$$\sigma_1(V_0 - V_1) = E(\sigma_1 - \sigma_0)[x\cos\alpha + y\sin\alpha].$$

Taking the limit as points tend to the boundary point on C_1:

$$\sigma_1[V_0^{C_1}(s) - V_1^{C_1}(s)] = E(\sigma_1 - \sigma_0)[x(s)\cos\alpha + y(s)\sin\alpha]. \quad (16)$$

Similarly one can prove that

$$\sigma_2[V_0^{C_2}(\tau) - V_2^{C_2}(\tau)] = E(\sigma_2 - \sigma_0)[x(\tau)\cos\alpha + y(\tau)\sin\alpha]. \quad (17)$$

In (20) the second integral vanishes and therefore it may be multiplied by an arbitrary constant, σ_2 say. The remainder of this equation is multiplied by σ_1, equation

(14) is multiplied by σ_0 and the resulting expressions are added to yield

$$\sigma_1 V_1^{C_1} + \sigma_0 V_0^{C_1} = \frac{1}{\pi}\oint_{C_1}\{[\sigma_1 V_1^{C_1}(s') - \sigma_0 V_0^{C_1}(s')]\frac{\partial \log r_{11}}{\partial n'} + [\psi_1^{C_1}(s') - \psi_0^{C_1}(s')]\frac{\partial \log r_{11}}{\partial s'}\}ds' + \frac{1}{\pi}\oint_{C_2}\{[\sigma_2 V_2^{C_2}(\tau') - \sigma_0 V_0^{C_2}(\tau')]\frac{\partial \log r_{12}}{\partial N'} + [\psi_2^{C_1}(\tau') - \psi_0^{C_2}(\tau')]\frac{\partial \log r_{12}}{\partial \tau'}\}d\tau'.$$

The above conditions of continuity allow to simplify this last relation to the form:

$$\sigma_1 V_1^{C_1} + \sigma_0 V_0^{C_1} = \frac{1}{\pi}\oint_{C_1}[\sigma_1 V_1^{C_1}(s') - \sigma_0 V_0^{C_1}(s')]\frac{\partial \log r_{11}}{\partial n'}ds' + \frac{1}{\pi}\oint_{C_2}[\sigma_2 V_2^{C_2}(\tau') - \sigma_0 V_0^{C_2}(\tau')]\frac{\partial \log r_{12}}{\partial N'}d\tau'. \quad (18)$$

With the help of (5) one obtains

$$\sigma_1 V_1^{C_1} + \sigma_0 V_0^{C_1} = \frac{1}{\pi}\oint_{C_1} G_1(s')\frac{\partial \log r_{11}}{\partial n'}ds' + \frac{1}{\pi}\oint_{C_2} G_2(\tau')\frac{\partial \log r_{12}}{\partial N'}d\tau'. \quad (19)$$

Adding (5) and (19) and dividing by $2\sigma_1$:

$$V_1^{C_1}(s) = \frac{1}{2\sigma_1}[G_1(s) + \frac{1}{\pi}\oint_{C_1} G_1(s')\frac{\partial \log r_{11}}{\partial n'}ds' + \frac{1}{\pi}\oint_{C_2} G_2(\tau')\frac{\partial \log r_{12}}{\partial N'}d\tau']. \quad (20)$$

Subtracting (5) from (20) and dividing by $2\sigma_0$:

$$V_0^{C_1}(s) = \frac{1}{2\sigma_0}[-G_1(s) + \frac{1}{\pi}\oint_{C_1} G_1(s')\frac{\partial}{\partial n'}\log r_{11}ds' + \frac{1}{\pi}\oint_{C_2} G_2(\tau')\frac{\partial}{\partial N'}\log r_{12}d\tau']. \quad (21)$$

Now subtract (21) from (20) and multiply by σ_1 to get

$$\sigma_1[V_1^{C_1}(s) - V_0^{C_1}(s)] = \frac{\sigma_1+\sigma_0}{2\sigma_0}G_1(s) + \frac{\sigma_0-\sigma_1}{2\pi\sigma_0}[\oint_{C_1} G_1(s')\frac{\partial \log r_{11}}{\partial n'}ds' + \oint_{C_2} G_2(\tau')\frac{\partial \log r_{12}}{\partial N'}d\tau'].$$

From (16):

$$E(\sigma_0-\sigma_1)[x(s)\cos\alpha + y(s)\sin\alpha] = \frac{\sigma_1+\sigma_0}{2\sigma_0}G_1(s) + \frac{\sigma_0-\sigma_1}{2\pi\sigma_0}[\oint_{C_1} G_1(s')\frac{\partial \log r_{11}}{\partial n'}ds' + \oint_{C_2} G_2(\tau')\frac{\partial}{\partial N'}\log r_{12}d\tau'].$$

Multiplying this last equation by $\frac{2\sigma_0}{\sigma_0+\sigma_1}$ and replacing $I = E\sigma_0$ yields

$$G_1(s) + \frac{\sigma_0-\sigma_1}{\pi(\sigma_0+\sigma_1)}[\oint_{C_1} G_1(s')\frac{\partial}{\partial n'}\log r_{11}ds' + \oint_{C_2} G_2(\tau')\frac{\partial}{\partial N'}\log r_{12}d\tau'] = \frac{2(\sigma_0-\sigma_1)}{\sigma_0+\sigma_1}I[x(s)\cos\alpha + y(s)\sin\alpha].$$

Differentiate w.r.to s and use (4):

$$F_1(s) + \frac{\sigma_0-\sigma_1}{\pi(\sigma_0+\sigma_1)}\frac{d}{ds}[\oint_{C_1} G_1(s')\frac{\partial}{\partial n'}\log r_{11}ds' + \oint_{C_2} G_2(\tau')\frac{\partial}{\partial N'}\log r_{12}d\tau'] = \frac{2(\sigma_0-\sigma_1)}{\sigma_0+\sigma_1}I[\dot{x}(s)\cos\alpha + \dot{y}(s)\sin\alpha].$$

Integration by parts and use of the Cauchy-Riemman relations

$$\frac{\partial}{\partial n}\log r_{11} = \frac{\partial}{\partial s}\theta_{11}, \qquad \frac{\partial}{\partial n}\log r_{12} = \frac{\partial}{\partial s}\theta_{12}$$

finally yields the integral equation

$$F_1(s) - \frac{\sigma_0-\sigma_1}{\pi(\sigma_0+\sigma_1)}[\oint_{C_1} F_1(s')\frac{\partial}{\partial n}\log r_{11}ds' + \oint_{C_2} F_2(\tau')\frac{\partial}{\partial n}\log r_{12}d\tau'] = \frac{2(\sigma_0-\sigma_1)}{\sigma_0+\sigma_1}I[\dot{x}(s)\cos\alpha + \dot{y}(s)\sin\alpha].$$

The second integral equation may be derived in a similar way as

$$F_2(\tau) - \frac{\sigma_0-\sigma_2}{\pi(\sigma_0+\sigma_2)}[\oint_{C_1} F_1(s')\frac{\partial}{\partial N}\log r_{21}ds' + \oint_{C_2} F_2(\tau')\frac{\partial}{\partial N}\log r_{22}d\tau'] = \frac{2(\sigma_0-\sigma_2)}{\sigma_0+\sigma_2}I[\dot{x}(\tau)\cos\alpha + \dot{y}(\tau)\sin\alpha].$$

References

[1] A.A. Ashour, S. Chapman, The magnetic field of electric currents in an unbounded plane sheet, uniform except for a circular area of different uniform conductivity, Geophys. J. R. astr. Soc. **10**, 31-44 (1965).

[2] S. Chapman, A.A. Ashour, Meteor geomagnetic effects, Smithonian Contributions to Astrophysics **8**, 181-197 (1965).

[3] A.A. Ashour, Electromagnetic induction in finite thin sheets, Quart. Journ. Mech. and Appl. Math. Res. **18**, 69-82 (1965).

[4] A. A. Ashour, The magnetic field of plane current sheet with different uniform conductivities in different parts with results for elliptic area, Geophys. J. R. astr. Soc. **22**, 401-416 (1971).

[5] A.A. Ashour, The magnetic field of an infinite plane current sheet uniform except for two circular insertions of different uniform conductivities, Geophys. J. R. astr. Soc. **83**, 1, 127-142 (1985).

[6] M.S. Abou-Dina, A.A. Ashour, A general method for evaluating the current system and its magnetic field of a plane current sheet, uniform except for a certain area of different uniform conductivity, with results for a square area, Il Nuovo Cimento **12 C**, 5, 304-311 (1989).

[7] M.S. Abou-Dina, A.A. Ashour, Exact solutions for certain two-dimensional problems of induction in thin non-uniform sheets, Geophys. Research **95**, 17547-17553 (1990).

[8] R. Cade, The integral equation solution of two-dimensional electrostatic problems involving circular cylinders, J. Inst. Maths. Applics. **25**, 211-230 (1980).

[9] A. Sellier, A slender dielectric body embedded in an arbitrary external potential, IMA Journal of Applied Mathematics **66**, 149-173 (2001).

[10] R. Shail, Some potential problems for slender tori, J. Inst. Maths. Applics. **24**, 303-325 (1979).

[11] R. Cade, Integral-equation perturbation theory for electrostatic torus problems with applied fields, IMA Journal of Applied Mathematics **36**, 59-84 (1986).

[12] R. Cade, On discontinuous solutions of the integral equations of electrostatics. IMA Journal of Applied Mathematics **55**, 205-220 (1995).

[13] P.E. Wannamaker, Advances in three-dimensional magnetotelluric modeling using integral equations, Geophysics **56**, 11, 1716-1728 (1991).

[14] D. Schieber, Transient eddy currents in thin metal sheets, IEEE Transactions on Magnetics **8**, 4, 355-361 (1972).

[15] P.J. Madle, W.A. Robinson, In situ method for measuring the permeability and resistivity of metal sheets, IEEE Transactions on Instrumentation and Measurement **24**, 4, 300-305 (1975).

[16] M. McIver, An inverse problem in electromagnetic crack detection, IMA Journal of Applied Mathematics **47**, 127-145 (1991).

[17] J.A. Reed, D.M. Byrne, , Using periodicity to control spectral characteristics of an array of narrow slots, Antennas and Propagation Society **4**, 2376-2379 (1997).

[18] S.J. Dong, G.P. Kelkar, Y. Zhou, Electrode sticking during micro-resistance welding of thin metal sheets, IEEE Transactions on Electronics Managing Packaging **25**, 4, 355-361 (2002).

[19] K. Gopalakrishnan, K. Goldberg, G.M. Bone, M.J. Zaluzec, R. Koganti, R. Pearson, P.A. Deneszczuk, Unilateral fixtures for sheet-metal parts with holes, IEEE Transactions on Automation Science and Engineering, **1**, 2, 110-120 (2004).

[20] Haitian Chen, U.K. Madawala, J. Tham, A low cost sensing technique for detecting defects on metal sheets, IEEE International Conference on Industrial Technology, 2286-2291 (2006).

[21] M.H. Dastjerdi, M. Rubesam, D. Ruter, J. Himmel, O. Kanoun, Non destructive testing for cracks in perforated sheet metals, 8-th International Multi-conference on Systems, Signals and Devices, 1-5 (2011).

[22] A. Erdélyi, Higher transcendental functions, v. 2, McGraw-Hill, New York (1953).

Doaa El-Sakout is a teaching assistant in the Department of Mathematics, Faculty of Science, Cairo University. She got a B. Sc. degree in Mathematics Education from Helwan University in 2004, a B. Sc degree in Mathematics from Cairo University in 2006 and an M. Sc. degree in Mathematics in June 2011. In June 2012 she got a PGD from the African Institute for Mathematical Sciences (AIMS) in South Africa, with a project in Computational Algebra and Enzyme Kinetics. She is now a Ph. D. student at the Institute of Petroleum Engineering, Heriot Watt University in Edinburgh, Scotland. She is currently working in Uncertainty Quantification. Her Ph. D. topic is in the general area of inference methods for porous media flows and is aimed at improving the ability to make reliable inference about such flows. She is interested in Electromagnetic Theory, Numerical Analysis, Fluid Mechanics, Ordinary and Partial Differential Equations, Complex Analysis, Special Functions, Quantum Computing, Dynamical Systems, Solitons, Non Linear Systems and Finite Element Method. This paper is extracted from the work on her Master thesis.

Ahmed Ghaleb is Emeritus Professor of Applied Mathematics at Cairo University since 1989. Head of the Department of Mathematics, Faculty of Science in 2002-2004. Ph. D. degree in Mathematics and Physics from the Faculty of Mathematics and Mechanics, Moscow State University in 1976 in the field of Relativistic Continuum Mechanics of Electromagnetic Media. Referee and editor of several journals, editor of "Mathematical Analysis, Wavelets and Signal Processing", Contemporary Mathematics n^0 190 (1995). Fulbright fellow in 1994-1995 at the Department of Civil Engineering and Operations Research, Princeton University, Princeton NJ, USA. His main research interests are: Continuum Mechanics of Electromagnetic Media and Boundary Integral Methods in the Theory of Thermoelasticity and Thermo-electromagnetoelasticity.

Moustafa Abou-Dina is Emeritus Professor of Applied Mathematics at Cairo University since 2002. He was awarded the Doctorat d'Etat degree in Fluid Mechanics from the I.M.G., University of Grenoble, France in 1983. He is a Referee of several local and international journals. Main research interests: Theory of Electro-Magnetism, Fluid Mechanics, Boundary Integral Methods in the Theories of Fluid Mechanics, Electro-Magnetic induction in thin sheets, Current sheets, Thermoelasticity and Thermo-electromagnetoelasticity.

Attia Ashour is Emeritus Professor of Applied Mathematics at Cairo University since 1989. Head of the Department of Mathematics, Faculty of Science, Cairo University for many years. He was awarded the Ph. D. degree in Mathematics from London University in 1948 and the D.Sc. in Mathematics from London University in 1967. Since 1954 a visiting scholar at many renowned scientific institutions, among which the National Center for Atmospheric Research, Boulder, Colorado, Geophysical Institute, University of Alaska, Geophysical Institutes in Gottingen, Braunschweig and Munich, Institut de Physique du Globe, Université de Paris. Fellow of the Royal Astronomical Society (R.A.S) since 1954 and Foreign Associate of RAS in 1978. Former President of the Mathematical and Physical Society of Egypt, President of the International Union of Geodesy and Geophysics (IUGG) between 1975-1979 and President of the International Center of Pure and Applied Mathematics, Nice, France, 1992-1996, and member of its Administrative Council, 1997-2000. He was awarded several Orders of Merit of Arts and Sciences of Egypt between 1966-1986, as well as Chevalier dans l'Ordre de La Palme Académique, from the French Government in 1985, the Medal of the African Mathematical Union in 1990 and Chevalier dans l'Ordre National de Mérite from the French President in 1995. The field of research of Attia Ashour is "Mixed Boundary Value Problems"with applications in Theoretical Physics and mainly in Theoretical Geomagnetism. He has lead an active school of research in these fields and several scientists have obtained their M.Sc. and Ph.D. degrees under his supervision. He is one of the few world experts on the Mathematical Theory of Electromagnetic Induction. Several theories in this mathematical field and in the applications carry the name of Attia Ashour.